



A self-sustaining monolithic photoelectrocatalytic/photovoltaic system based on a WO₃/BiVO₄ photoanode and Si PVC for efficiently producing clean energy from refractory organics degradation

Qingyi Zeng^{a,b}, Lai Lyu^a, Yaowen Gao^a, Sheng Chang^a, Chun Hu^{a,*}

^a Key Laboratory for Water Quality and Conservation of the Pearl River Delta, Ministry of Education, Institute of Environmental Research at Greater Bay, Guangzhou University, Guangzhou, 510006, PR China

^b School of Environmental Science and Engineering, Shanghai Jiao Tong University, No.800 Dongchuan Rd, Shanghai 200240, PR China

ARTICLE INFO

Keywords:

Wastewater treatment
Electricity
Hydrogen
WO₃/BiVO₄photoanode
Sunlight

ABSTRACT

A novel self-sustaining monolithic photoelectrocatalytic/photovoltaic (SMPP) system is constructed with a FTO-glass-based WO₃/BiVO₄ photoanode, which was prepared by coating BiVO₄ on WO₃ nanoplate array using simple wet chemical methods, a rear Si photovoltaic cell (PVC) and a counter Pt-black/Pt cathode. The optimum SMPP system shows an efficient and stable degradation of tetracycline hydrochloride with a rate constant 0.75 h⁻¹, and yields an open circuit voltage 1.35 V, a short circuit current 2900 μA cm⁻², a power density 1112 μW cm⁻², which is nearly 14 times that of the ultimate conventional photocatalytic fuel cell to date, and a hydrogen generation rate 52.6 μmol h⁻¹ cm⁻². This outstanding performance should be due to the efficient electron/hole separation and light exploitation, because, under stimulated sunlight illumination, the front WO₃/BiVO₄ photoanode absorbs short-wavelength photons and generates electron/hole pairs, in which the photogenerated holes can oxidize organics, while the rear Si PVC captures the transmitting longer-wavelength photons to generate photovoltage that drives photogenerated electrons to the cathode for reducing H⁺ to H₂ and generating electricity in the external-circuit. The results also demonstrate that various refractory organics can be efficiently decomposed along with the production of electricity and hydrogen by the SMPP system. This work provides a more efficient way to dispose organics and simultaneously produce clean energy than conventional technologies and serves well as a promising technology for wastewater recycling.

1. Introduction

Water pollution is a severe crisis that is threatening the life of people from all around the world, and brings a great challenge for the sustainable development of human beings. The situation is becoming more severe because of the release of hazardous and bio-refractory organic pollutants, such as dyes, pharmaceutical compounds, etc., which lead to persistent contamination to waters [1,2]. On the other hand, organic wastewater is a potential renewable resource because the contained organics are rich in chemical energy, e.g. one mole phenol can release about 3050.6 kJ mol⁻¹ heat when complete mineralized. However, conventional sewage disposal technologies, such as biological treatment technology, advanced oxidation technology and membrane separation technology, mainly aim to remove pollutants while the energy consumption and energy recovery are rarely considered [3]. Therefore, seeking low-cost and high efficiency approaches to eliminating hazardous pollutants and simultaneously recycle organics' chemical

energy has become a key issue of global concern.

To increase the energy benefit, photocatalytic fuel cell (PFC) was developed to converting chemical energy of organic pollutants (fuel) into electricity accompanied with organic compounds degradation at the expense of incident light [4–12]. This PFC system is more advantage than traditional microbial fuel cell (MFC), which is a widely studied and promising technology for the purpose of using bacteria as the catalysts to oxidize various substrates and recover electricity [13], because the fast and direct transportation process of photogenerated electrons in photocatalytic process replaces the slow and complex biochemical electron transfer process [4,5,8]. In previous works, PFCs were based on a single photoanode such as TiO₂ films for fuel oxidation reaction and a counter Pt cathode for oxygen reduction reaction (ORR), and the electricity output performance was proved by using many kinds of organic substrates [4–7]. Further developed PFCs were designed in a dual photoelectrode configuration by using p-type semiconductor photo-cathode such as Cu₂O films to replace passive Pt cathode for ORR to

* Corresponding author.

E-mail address: huchun@gzhu.edu.cn (C. Hu).

<https://doi.org/10.1016/j.apcatb.2018.07.005>

Received 18 April 2018; Received in revised form 29 June 2018; Accepted 2 July 2018

Available online 06 July 2018

0926-3373/ © 2018 Elsevier B.V. All rights reserved.

enhance the energy conversion efficiency, because the mismatched Fermi levels between photoanode and photocathode facilitated the charge transfer between the photoelectrodes [8–12]. For example, Chen et al. [8] reported a dual-photoelectrode PFC based on a WO_3/W photoanode and $\text{Cu}_2\text{O}/\text{Cu}$ photocathode that showed a short circuit current density (J_{sc}) of $205 \mu\text{A cm}^{-2}$ and an open circuit voltage (V_{oc}) of 0.33 V for degrading phenol under Air Mass (AM) 1.5 illumination, which was outperformed the single photoanode PFC consisting of WO_3/W photoanode and Pt foil. Zhang et al. [12] recently reported aPFC based on aW-doped BiVO_4 photoanode and a polyterthiophene photocathode yielded a power density (P_{max}) of only $82 \mu\text{W cm}^{-2}$, which outperformed dual-photoelectrode PFCs previously reported. Despite the feasibility of simultaneous wastewater treatment and energy recovery of organic wastes was proved using a simple PFC system, the electricity output efficiency and energy benefit for solar light exploitation in these PFCs were limited by the small inner bias of Fermi level difference and the separated light illumination of photoanode and photocathode.

In this work, for the first time we report a novel self-sustaining monolithic photoelectrocatalytic/photovoltaic (SMPP) system made of asubtransparent $\text{WO}_3/\text{BiVO}_4$ photoanode, a rear Si photovoltaic cell (PVC) and a counter Pt-black/Pt cathode for efficient organic degradation and simultaneous electricity and hydrogen production using sunlight. In this SMPP system, the $\text{WO}_3/\text{BiVO}_4$ photoanode, prepared by decorating BiVO_4 on WO_3 nanoplate array film using simple wet chemical methods, is favorable in PC degradation of organics because of the quasi-type II heterostructure, good visible-light absorption of BiVO_4 and charge transfer property of WO_3 . A widely-used and low-cost single-junction monocrystal Si PVC, which exhibited an absorption spectrum complementary to the $\text{WO}_3/\text{BiVO}_4$ photoanode, is chosen as a bias supplier to efficiently utilize solar energy across the whole spectral range. When the sunlight shines the SMPP system from the photoanode side, the $\text{WO}_3/\text{BiVO}_4$ heterostructure mainly absorbs short-wavelength photons and generates electron/hole pairs, in which the photo-generated holes have enough energy ($\sim 2.4 \text{ eV}$ vs. NHE) to oxidize organics. The transmitting longer-wavelength photons are captured by the rear Si PVC to generate photovoltage that drive photogenerated electrons to the Pt-black/Pt cathode for reducing H^+ to H_2 and generating electricity in the exterior circuit. Based on this rational design, the optimal SMPP system shows an efficient and stable degradation of tetracycline hydrochloride, which used as a mode pollutant, with a rate constant of 0.75 h^{-1} , and yields an open circuit voltage (V_{oc}) of 1.35 V, a short circuit current (J_{sc}) of $2900 \mu\text{A cm}^{-2}$, a power density (P_{max}) of $1112 \mu\text{W cm}^{-2}$, and a hydrogen generation rate of $52.6 \mu\text{mol h}^{-1} \text{ cm}^{-2}$ during the degrading operation. The electricity output of the SMPP system is nearly 14 times that of theultimate reported PFC to date. Various refractory organics can be also efficiently decomposed along with the production of electricity and hydrogen by the SMPP system. This work provides a more efficient way to wastewater treatment and simultaneously produce clean energy using sunlight than conventional technologies.

2. Experimental

2.1. Preparation of the WO_3 nanoplate film

The WO_3 film was prepared via a simple wet chemical method based on peroxotungstate reduction reaction [14]. The purchased FTO coated glass substrate ($13 \Omega \text{ cm}^{-1}$) was cut in $3 \times 3 \text{ cm}^2$ and washed ultrasonically in acetone and deionized (DI) water for 30 min, sequentially. The precursor solution was prepared as follow: 0.6 g H_2WO_4 , 0.28 g $(\text{NH}_4)_2\text{C}_2\text{O}_4$, 18 mL HCl (37%) and 16 mL H_2O_2 (37%) was dissolved in 66 mL DI water in sequence, and then 60 mL of ethanol were added into this solution under strong agitation to obtain the precursor solution. The FTO glass was dipped into this precursor solution with the FTO side adown, and then kept at 85°C in a constant temperature bath for 3 h

and then cooled naturally. The as-prepared film was rinsed with DI water and dried at 80°C for 5 h, and then annealed at 500°C for 3 h to obtain the WO_3 film.

2.2. Preparation of $\text{WO}_3/\text{BiVO}_4$ photoanode

The preparation of $\text{WO}_3/\text{BiVO}_4$ photoanodes were using spin-coating processes based on the reaction of bismuth nitrate with peroxovanadate [15]. Before the preparation process, the bismuth nitrate solution was prepared by dissolving 2.43 g $\text{Bi}(\text{NO}_3)_3 \cdot 5\text{H}_2\text{O}$ in 100 mL 2 M acetic acid solution. For the peroxovanadate solution, 1.77 g NH_4VO_3 was dissolved in 100 mL 150 mM H_2O_2 solution by ultrasonic resulting a saffron yellow solution (pH 7.4). In a typical preparation process, 0.5 mL bismuth nitrate solution was dropped on the WO_3 film following with a spin rate of 2000 r.p.m. for 15 s, and then 0.5 mL peroxovanadate solution was deposited on it under the same spin-coating condition. This process was named one spin-coating cycle, and typical cycles were 15 times. Then the film was rinsed with DI water and dried at 50°C for 10 h, and then annealed at 450°C for 3 h to obtain the $\text{WO}_3/\text{BiVO}_4$ photoanode.

2.3. Characterization

The morphologies and microstructures of the samples were investigated via scanning electron microscopy (SEM, Sirion200, Philips, Netherlands) at an acceleration voltage of 5 kV. The crystal phase of the samples was characterized via X-ray diffraction (XRD, AXS-8 Advance, Bruker, Germany). The UV-vis absorption spectra of the samples were obtained using a UV-vis photospectrometer (TU-1901, PGeneral Instrument Inc., China).

LSV test was performed in a three-electrode system with SCE as the reference, Pt foil as the counter-electrode, and the $\text{WO}_3/\text{BiVO}_4$ photoanode as the working electrode (front-side illumination) in an electrolyte consisting of 0.1 M Na_2SO_4 solution, controlled by an electrochemical workstation (CHI 660c, CH Instruments, Inc., USA). A 300-W Xe lamp (PerfectLight, China) with an AM 1.5 filter was used for simulated solar light illumination (light density: 100 mW cm^{-2}). IPCE was measured by a system operated with a monochromator (Zolix, China), a 500 W xenon arc lamp, a calibrated silicon photodetector, and a power meter.

2.4. SMPP system for degrading tetracycline hydrochloride

The SMPP system was constructed by attaching commercial Si photovoltage system (Si PVC, function area $4 \times 2 \text{ cm}^2$, Shenzhou New Energy Development Co., Ltd., Shanghai, China) at the rear of $\text{WO}_3/\text{BiVO}_4$ photoanode, and using a Pt-black/Pt electrode as cathode. The $\text{WO}_3/\text{BiVO}_4$ photoanode was connected with the positive pole of Si PVC and sealed with Si PVC by silicone rubber as a monolithic photoelectrode. 0.1 M Na_2SO_4 solution containing 10 mg L^{-1} tetracycline hydrochloride was used as the mode wastewater. The degradation tests were carried out in a homemade rectangular quartz reactor with 100 mL mode wastewater. The light illumination was AM 1.5 (100 mW cm^{-2}). The illumination area was 8 cm^2 . The degradation rate was analyzed with a spectrophotometer (UH4150, Hitachi, Japan) at wavelength of 357 nm. The current of the SMPP system was recorded by the electrochemical station (Zennium, ZAHNER, Germany). The effect of wavelength of incident light on the performance of SMPP system was carried out by applying a 300-W Xe lamp (PerfectLight, China) with various optical filter (350, 380, 405, 420, 450, 500, 550, 600 nm) as light source.

Various refractory organics, such as methylene blue (MB), congo red (CR), phenol, bisphenol A (BPA), p-chlorophenol and oxytetracycline (OTC), and other organics, such as urea, dimethyl formamide (DMF), acetic acid and mannitol, were further used as model organic pollutants to evaluate the performance of the SMPP system. The concentration of

each refractory organic was 10 mg L^{-1} , and it was 20 mg L^{-1} for other organics. The removal ratios of MB and CR were analyzed by spectrophotometer (UH4150, Hitachi, Japan), and other organics were analyzed by a high performance liquid chromatography (HPLC, 1260 Infinity II, Agilent Technologies, USA). The variation of total organic carbon (TOC) of the simulative wastewater was tested using a TOC analyzer (TOC-L CPH CN200, Shimadzu, Japan).

The hydrogen evolution during degradation of organics was measured in a quartz device (LabSolar-IIIAG, Perfect Light, China) which includes the gas collection system and reactor. This device is connected with a vacuum pump (2TW-6 G, Tingwei, China), a low-constant-temp bath (DC-2006, CNSHP, China), and a gas chromatograph (GC, GC-2010plus, Shimadzu, Japan). Before the test, the quartz device is vacuumized by vacuum pump to remove the dissolved gas of the mode wastewater and the air in the device. The temperature of the low-constant-temp bath is -2°C to prevent the water vapour from the electrolyte into the gas collection system. During the test, a certain amount gas in the gas collection system is sent into the GC system to analysis the amount of H_2 after certain interval.

3. Results and discussion

3.1. Characterization of the $\text{WO}_3/\text{BiVO}_4$ photoanode

The morphology and microstructure of the as prepared WO_3 film and $\text{WO}_3/\text{BiVO}_4$ photoanode were revealed by the scanning electron microscopy (SEM) analysis as shown in Fig. 1. The WO_3 photoanode shows a plate-like morphology with quasi-vertically oriented nanoplate arrays and a film thickness of $\sim 870 \text{ nm}$ (Fig. 1a). The thicknesses of the WO_3 nanoplates are $60\text{--}110 \text{ nm}$. In the case of nanostructured WO_3 substrate, it provides a large surface area to load more amount of

BiVO_4 , therefore increasing the light absorption and the charge transfer between BiVO_4 layer and WO_3 substrate. The $\text{WO}_3/\text{BiVO}_4$ photoanode shows a porous morphology with nanoporous BiVO_4 coated WO_3 nanoplates with a film thickness of $\sim 950 \text{ nm}$ (Fig. 1b). This porous morphology provide fantastic nanostructure for improving interfacial reaction kinetics.

The crystallographic features of the as prepared photoanodes were investigated by X-ray diffraction (XRD) as shown in Fig. 1c. In the case of the WO_3 photoanode, the diffraction peaks at 23.3° , 23.8° , and 24.6° are observed corresponding to (002), (020), and (200) planes for the monoclinic WO_3 (JCPDS 43-1035), which is known to show the highest photocatalytic effect than other crystal phases [16]. The intensified (200) diffraction peak indicates the nanostructured WO_3 photoanode has a preferential orientation of [200]. For the $\text{WO}_3/\text{BiVO}_4$ photoanode, the diffraction peak at 18.5° and the intensified peak at 29.4° are ascribed to monoclinic BiVO_4 (JCPDS 14-0688), which is most active structure for photocatalysis [17]. The optical behaviors of the WO_3 and $\text{WO}_3/\text{BiVO}_4$ photoanodes were characterized by UV–vis absorbance spectra (Fig. 1d). The bare WO_3 shows an absorption edge of $\sim 471 \text{ nm}$ which is corresponding with its band gap energy [18]. After decorating with BiVO_4 , the $\text{WO}_3/\text{BiVO}_4$ photoanode shows an absorption edge of $\sim 518 \text{ nm}$ indicating that the absorption range of WO_3 is improved by coupling of BiVO_4 with a smaller band gap energy [19].

Fig. 2a compares the typical chopped linear sweep voltammetry (LSV) plots of the WO_3 and $\text{WO}_3/\text{BiVO}_4$ photoanodes under Air Mass (AM) 1.5 illumination. The photocurrent density (J) of the WO_3 photoanode is about 1.16 mA cm^{-2} at 0.6 V vs. SCE . After decorated BiVO_4 on the WO_3 nanoplate film, the $\text{WO}_3/\text{BiVO}_4$ photoanode exhibits a noticeable improvement in photocurrent response with a J of 2.35 mA cm^{-2} at 0.6 V vs. SCE , which represents a 102% improvement compared to the WO_3 photoanode. The comparison of the incident-photo-

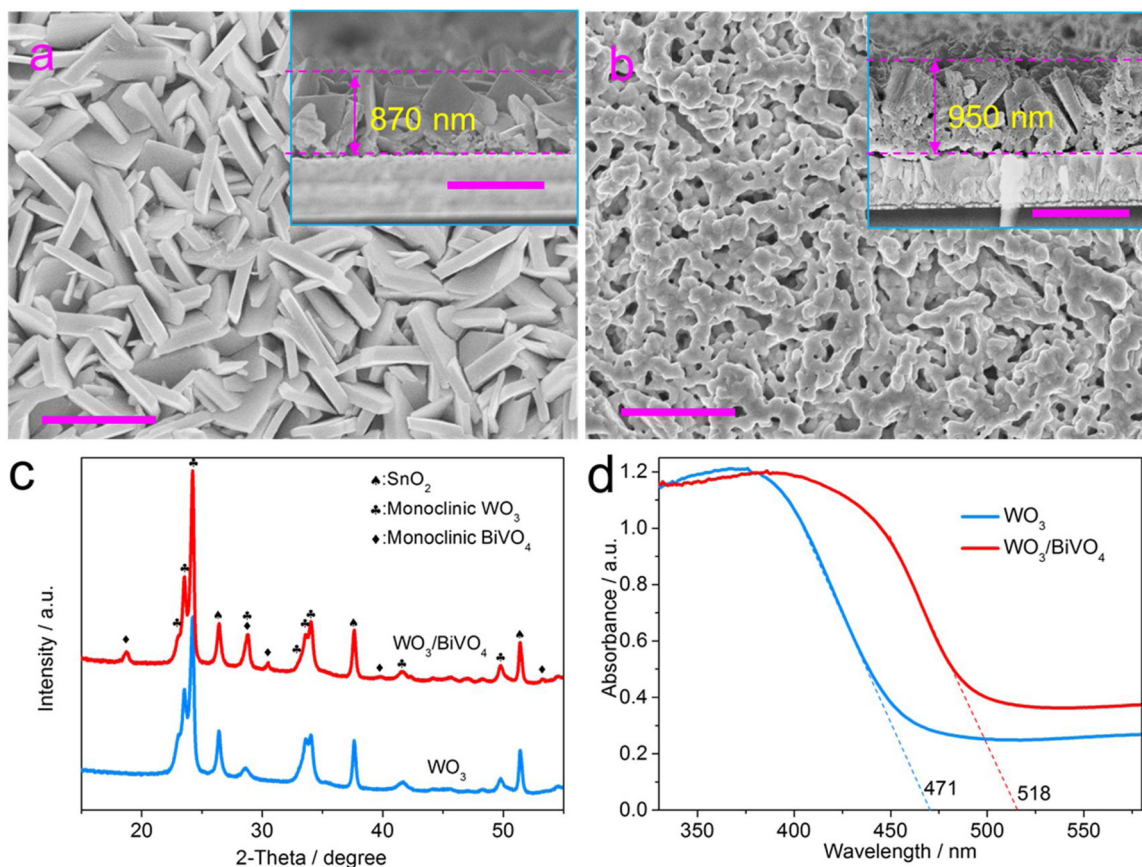


Fig. 1. SEM images of (a) WO_3 and (b) $\text{WO}_3/\text{BiVO}_4$ photoanodes. Inserts are the corresponding cross-section images. All the scale bars are $1 \mu\text{m}$. (c) XRD patterns and (d) UV–vis absorbance spectra of the as prepared photoanodes.

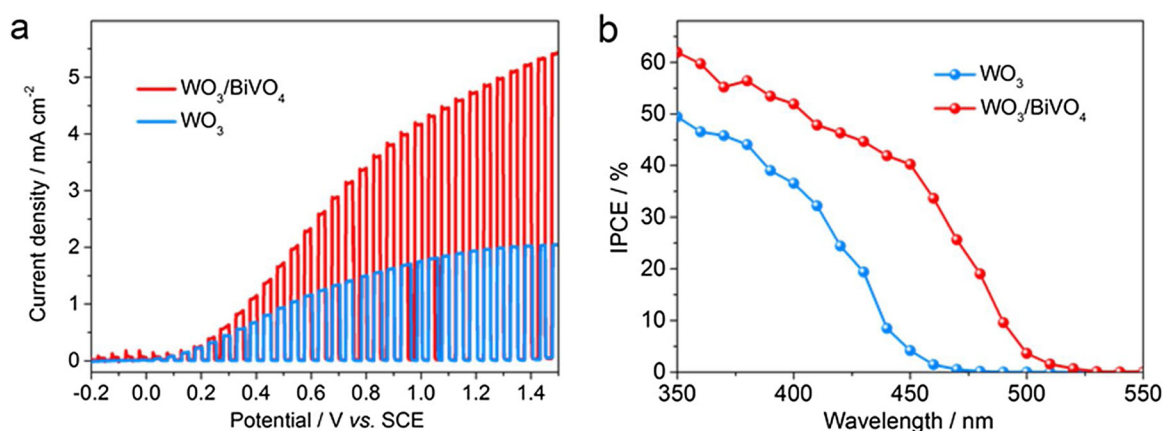


Fig. 2. (a) Chopped LSV plots and (b) IPCE spectra (at 0.6 V vs. SCE) of the WO₃ and WO₃/BiVO₄ photoanodes tested in 0.1 M Na₂SO₄ under AM 1.5 illumination, scan rate 5 mV s⁻¹.

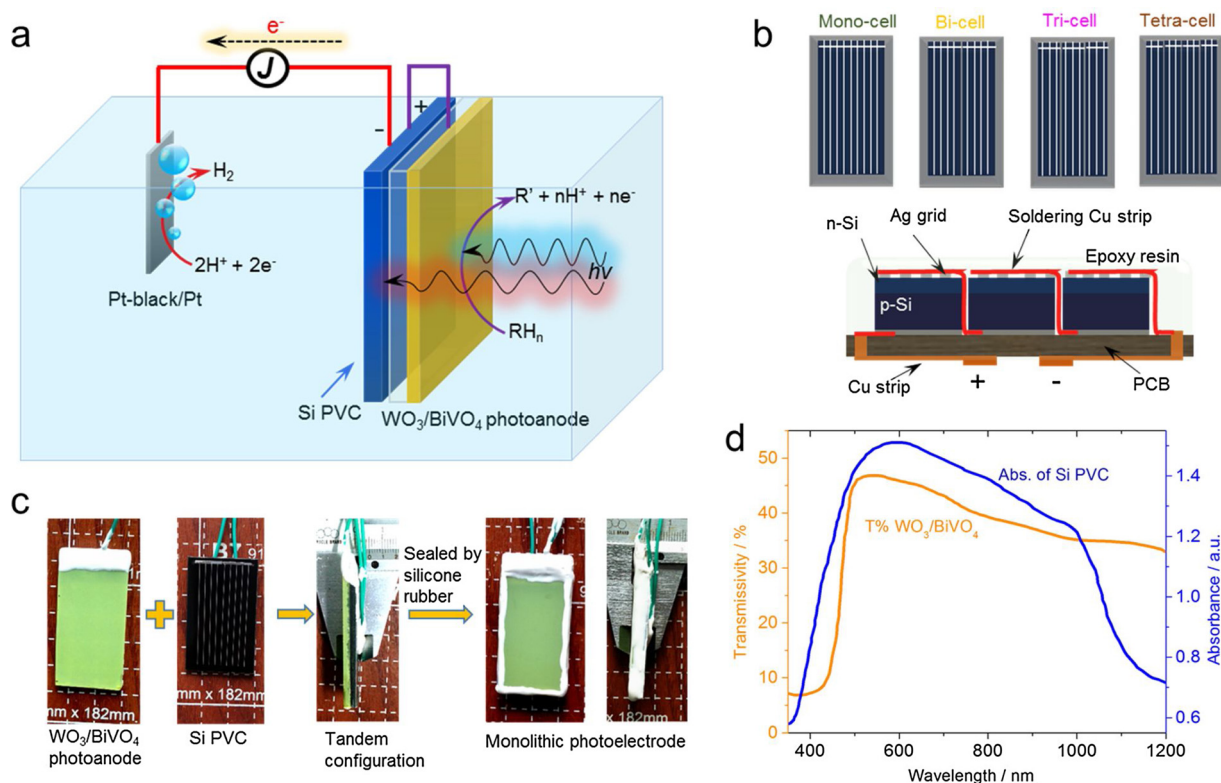


Fig. 3. (a) Schematic illustration of the SMPP system for simultaneous organic pollutant degradation, hydrogen generation and electricity production. (b) Schematic illustration of four types of Si PVC arrays and the structure of tri-cell. (c) Digital photos show the construction of the monolithic photoelectrode. (d) The light absorption of Si PVC and light transmission of the WO₃/BiVO₄ photoanode.

to-current (IPCE) behaviors of the two photoanodes shown in Fig. 2b further indicates that the absorbed photons can be converted into photocurrent more efficiently in the WO₃/BiVO₄ photoanode, which also shows a more extended responsive range over to 520 nm. It is reported that BiVO₄ has more negative conduction band edge (CB) and valence band edge (VB) than both that of WO₃ [20]. The heterostructure of WO₃/BiVO₄ photoanode consequently is favorable for both the transport of photogenerated electrons from the CB of BiVO₄ to that of WO₃ and photogenerated holes from the VB of WO₃ to that of BiVO₄ because of the quasi type-II interfacial band structure, in turn suppressing the recombination of electron-hole pairs because of the strong thermodynamic effect [21]. Furthermore, the good charge transport property of WO₃ (~12 cm² V⁻¹ s⁻¹) ensures the photogenerated electrons readily transfer to the FTO substrate [22]. Therefore, the WO₃/BiVO₄

photoanode shows marvelous improvement in the photocurrent response compared to the bare WO₃ photoanode, suggesting it has highly photoactivity in photoelectrocatalytic (PEC) wastewater treatment.

3.2. Establishment of the SMPP system

Solar driven wastewater treatment by photoelectrodes is a promising and eco-friendly way to remediate waters [23,24]. As can be seen from the LSV plots as shown in Fig. 2, the photo-to-current efficiency is increased by raising the bias potential, which means the separation of photogenerated electron-hole pairs is enhanced along with the increase of bias potential. Therefore, traditional PEC systems for degrading organics always applied an external bias potential to improve degradation performance [25]. In addition, the degradation of organics

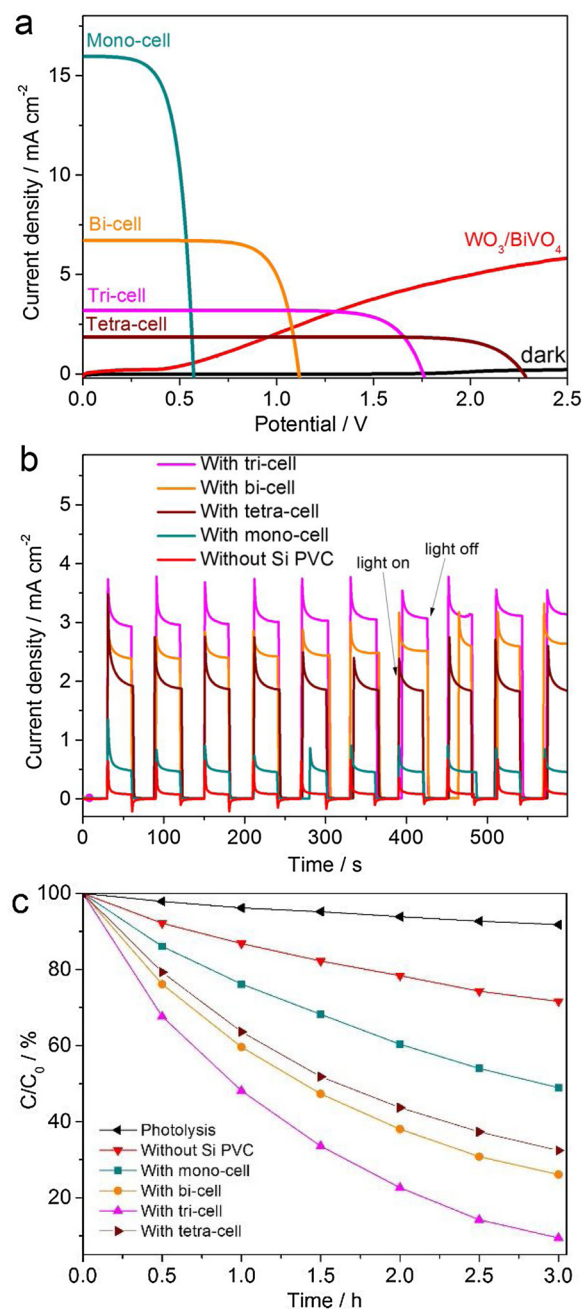


Fig. 4. (a) The J - V curves of various Si PVC arrays tested under AM 1.5 illumination filtered by the semi-transparent front WO₃/BiVO₄ photoanode, and the J - V curves of the WO₃/BiVO₄ photoanode tested in a two-electrode configuration with a Pt-black/Pt cathode in 0.1 M Na₂SO₄ solution under AM 1.5 illumination; (b) the chopped J - t curves of SMPP systems with various Si PVC arrays tested in 0.1 M Na₂SO₄ solution under AM 1.5 illumination. (c) Degradation of tetracycline hydrochloride by direct photolysis, and SMPP systems with various Si PVC arrays under AM 1.5 illumination.

mainly caused by the oxidation of photogenerated holes and hydroxyl radicals. The photogenerated electrons are transferred to the cathode to reduce water to hydrogen ($2\text{H}^+ + 2\text{e}^- \rightarrow \text{H}_2\uparrow$, $E^\circ(\text{H}^+/\text{H}_2) = 0\text{ V}$ vs. SHE at pH 0) or oxygen to superoxide anions ($\text{O}_2 + \text{e}^- \rightarrow \text{O}_2^{\cdot-}$, $E^\circ(\text{O}_2/\text{O}_2^{\cdot-}) = -0.33\text{ V}$ vs. SHE for a standard state of 1 bar O₂) [26]. Actually, the oxidation capacity of superoxide anions is lower than photogenerated holes and hydroxyl radicals, and the formation of superoxide anions always needs aeration condition to keep sufficient oxygen concentration [27,28]. Therefore, under normal conditions, the hydrogen generation is more preferential and energy-saving than reduce oxygen

when degrading organics. As shown in Fig. 3a, a multi-functional, self-sustaining monolithic photoelectrocatalytic/photovoltaic (SMPP) system is proposed for simultaneous wastewater treatment and hydrogen generation using sun light by combining a WO₃/BiVO₄ photoanode, a rear silicon photovoltaic system (Si PVC) and a Pt black/Pt cathode in tandem. When illuminating sun light from the photoanode side, the WO₃/BiVO₄ photoanode absorbs relatively short wavelength light to photocatalytic degradation of organics, and the rear Si PVC absorbs relatively long wavelength transmission light to generate bias potential to facilitate the transfer of photogenerated electrons in WO₃/BiVO₄ photoanode to the Pt black/Pt cathode to generate hydrogen. Obviously, this system not only resolves the supplying issue of bias potential but also enhances the exploitation of the solar spectrum.

In this work, monocrystal single-junction Si PVC was chosen as the bias potential supplier because it is a very efficient, commercial photovoltaic device with much lower cost than III-V semiconductors and multi-junction PVCs, and with superior stability compared to dye sensitized solar cell and perovskite solar cell to date [29]. The output voltage of the PVC is critical to determine the separation of photogenerated electron-hole pairs in the photoanode as a high bias potential usually drives a high PEC current density. To achieve the optimized wastewater treatment performance by the SMPP system, four types of Si PVC arrays (Fig. 3b) were applied in this work. The configurations of the Si PVC arrays are shown in Fig. 3b. For instance, the tri-cell (i.e., an array of three single-junction monocrystal Si PVCs interconnected in series) composes of three $0.67 \times 4\text{ cm}^2$ monocrystal single-junction Si PVCs that are adhered to the printed circuit board (PCB) side by side, and connected in series circuit by soldering copper strip, and sealed by epoxy resin. The WO₃/BiVO₄ photoanode and the rear Si PVC were designed as a monolithic photoelectrode, and the preparation flow is shown in Fig. 3c. The Si PVC is adhered to the back of the WO₃/BiVO₄ photoanode and sealed by silicone rubber. The WO₃/BiVO₄ photoanode is connected with the positive pole of the Si PVC. The monolithic photoelectrode has a function area of $4 \times 2\text{ cm}^2$. This monolithic configuration can simultaneously maximize light utilization and minimize complexity of the device. Furthermore, this integrated configuration can be easily used in practical wastewater treatment to construct an independent equipment.

Fig. 3d shows the light transmissivity of WO₃/BiVO₄ photoanode and the light absorbance of Si PVC. Higher than 35% light in the range of 500 nm–1200 nm can transmit the WO₃/BiVO₄ photoanode and the Si PVC has intensive light absorption in the range of 500 nm–1000 nm, which means that the WO₃/BiVO₄ photoanode and Si PVC have complementary absorption of light, suggesting the exploitation of sun light can significantly enhanced in the SMPP system and Si PVC can function at the rear of WO₃/BiVO₄ photoanode, ensuring the SMPP system operating well under only sun light illumination.

3.3. Performance of the SMPP system

The theoretical current density that can be achieved in a SMPP system can be determined by the intersection point of the current-voltage (J - V) characteristics of WO₃/BiVO₄ photoanode and Si PVC, which are obtained in a two-electrode configuration with a counter electrode of Pt-black/Pt cathode. Fig. 4a shows the resulted J - V characteristics of WO₃/BiVO₄ photoanode and various Si PVC arrays (with the shelter of WO₃/BiVO₄ photoanode) under AM 1.5 light illumination. It can be seen that the theoretical current densities of the SMPP systems ranked in: tri-cell > bi-cell > tetra-cell > mono-cell. This result indicates that the current density of a SMPP system with a certain photoanode depends on both open-circuit potential (V_{oc}) and short-circuit current density (J_{sc}) of the rear Si PVC. The SMPP system with a tri-cell Si PVC may have the highest theoretical current density of $\sim 3.13\text{ mA cm}^{-2}$.

Fig. 4b shows the chopped current-time (J - t) curves of the constructed SMPP systems with various Si PVC arrays. It can be seen that the photocurrent density of the system without Si PVC (constructed

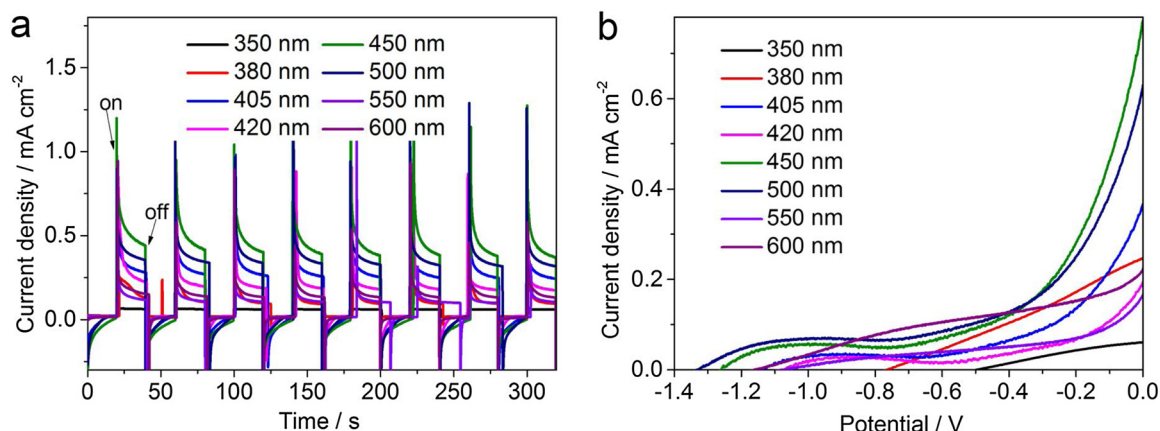


Fig. 5. (a) Chopped $J-t$ curves and (b) $J-V$ curves of SMPP system tested in 0.1 M Na_2SO_4 solution under incident-light of various wavelength (300-W Xe lamp with various filters).

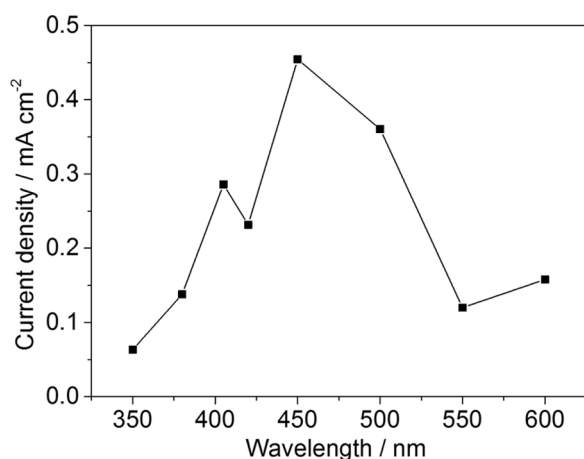


Fig. 6. The current density of SMPP system under incident-light of various wavelength.

with the $\text{WO}_3/\text{BiVO}_4$ photoanode and Pt-black/Pt cathode) is the lowest value of only $\sim 0.092 \text{ mA cm}^{-2}$. When using a mono-cell Si PVC, the SMPP system shows an improved photocurrent density of $\sim 0.53 \text{ mA cm}^{-2}$, which is ~ 5.76 -fold of that of the system without Si PVC. However, the SMPP system with a tri-cell exhibits the highest photocurrent density of $\sim 2.98 \text{ mA cm}^{-2}$, which is ~ 32.4 -fold of that of the PEC system without Si PVC. The photocurrent densities of the SMPP systems with various Si PVC arrays are in accordance with the theoretical values from Fig. 4a. This result indicates that attaching a Si PVC at the rear of $\text{WO}_3/\text{BiVO}_4$ photoanode in tandem can facilitate the separation of photogenerated electron-hole pairs in $\text{WO}_3/\text{BiVO}_4$ photoanode, resulting in a marvelous improvement in PEC performance.

To evaluate the degradation efficiency of the SMPP system, tetracycline hydrochloride was selected as a model substrate, because tetracycline hydrochloride is a widely used broad-spectrum antibiotic which is toxic and bio-refractory, and its release into the waters is harmful to the eco-system and can cause persistent damage [30]. As shown in Fig. 4c, the degradation efficiency of the direct photolysis was much slower than the other processes. Photolysis of tetracycline hydrochloride with simulated sunlight alone resulted in only 8.2% removal ratio after 3 h. After applied a PEC system constructed of $\text{WO}_3/\text{BiVO}_4$ photoanode and Pt-black/Pt cathode (without Si PVC), the removal ratio increased to 28.3%, which indicates that the photocatalytic process improves the degeneration of tetracycline hydrochloride. However, the SMPP systems show further improved degradation efficiency, and the SMPP system with a tri-cell shows the highest removal ratio of 90.6% after 3 h operation, which is about 220% improvement

compared to the PEC system without Si PVC. The ranking of the calculated rate constant of various processes was SMPP system with tri-cell (0.75 h^{-1}) > SMPP system with bi-cell (0.51 h^{-1}) > SMPP system with tetra-cell (0.43 h^{-1}) > SMPP system with mono-cell (0.27 h^{-1}) > PEC system without Si PVC (0.14 h^{-1}) > photolysis (0.038 h^{-1}). The rate constant of the SMPP system with tri-cell is about 5.36-fold of the PEC system without Si PVC, which indicates that using a rear Si PVC to complementarily using the transmitted solar light to supply a bias potential brings about a marvelous improvement in degenerating organics. From the result of Fig. 4a, the increasing performance of the PEC system < SMPP system with mono-cell < SMPP system with bi-cell < SMPP systems with tri-cell may be attributed to the increased potential from the rear Si PVC array. However, the decreased performance of the SMPP system with tetra-cell may be restricted by the small short circuit current density of the tetra-cell. All these results also reveal that the SMPP system with tri-cell has the optimum performance. Therefore, without specific mention, the SMPP system mentioned in the following text is constructed with the $\text{WO}_3/\text{BiVO}_4$ photoanode, tri-cell Si PVC (which is described as Si PVC in the following context for simplicity) and Pt-black/Pt cathode.

The effect of wavelength of incident light on the performance of SMPP system was further evaluated (Figs. 5 and 6). As shown in Fig. 6, the tendency of photocurrent density of SMPP system is approximately volcanic type. The relatively low photocurrent density under short wavelength light, such as 350 and 380 nm, should be due to the strong absorption of $\text{WO}_3/\text{BiVO}_4$ photoanode (Fig. 3d), which hides the response of rear Si PVC. Therefore, the bias potential is too low (Fig. 5b) to drive the photogenerated charge transportation. However, under a relatively long wavelength light, such as 550 and 600 nm, the $\text{WO}_3/\text{BiVO}_4$ photoanode has a weak light absorption to generate enough photogenerated charges, although the bias potential is relatively high (Fig. 5b). Only under a mediate wavelength light, such as 450 nm, the photocurrent density is relatively high, which should be attribute to the dual response of the front $\text{WO}_3/\text{BiVO}_4$ photoanode and rear Si PVC (Fig. 3d). These results indicate that the operation of the SMPP system needs both the $\text{WO}_3/\text{BiVO}_4$ photoanode and Si PVC activated under light illumination, and the sunlight that has a wide range of wavelength is an idea light source to drive the SMPP system.

Fig. 7a shows the photoelectric conversion performance of the SMPP system during degrading tetracycline hydrochloride under AM 1.5 illumination. The V_{oc} , J_{sc} and maximum power output density (P_{max}) of the SMPP system were $\sim 1.35 \text{ V}$, $\sim 2900 \mu\text{A cm}^{-2}$, and $1112 \mu\text{W cm}^{-2}$, respectively. Compared with the reported self-sustained PEC systems for wastewater treatment, such as dual-photoelectrode photocatalytic fuel cell (PFC), our SMPP system possesses significant improvement in electricity output (Table 1). A P_{max} of $82 \mu\text{W cm}^{-2}$ in the PFC with W-doped BiVO_4 (W:BiVO₄) photoanode and polyterthiophene

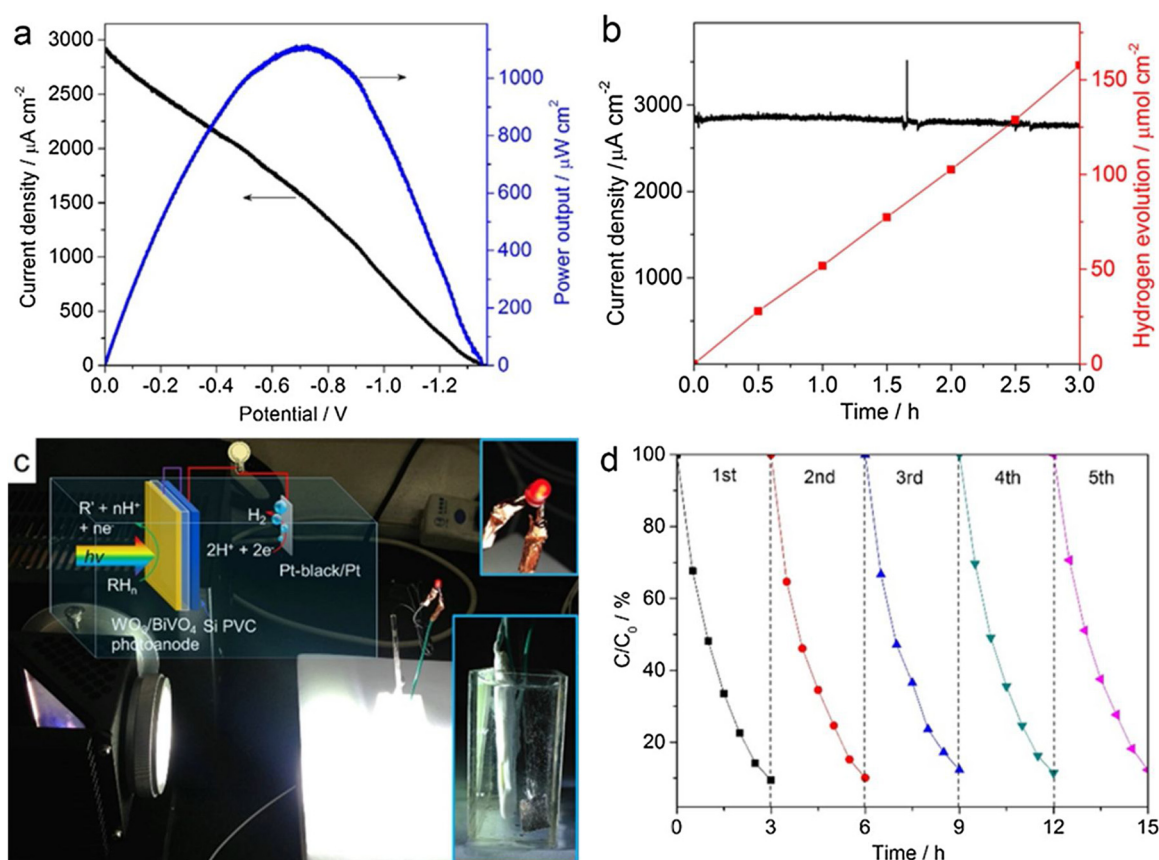


Fig. 7. (a) *J*-*V* curve and power output curve; (b) *J*-*t* curve and hydrogen evolution rate of SMPP system during degrading tetracycline hydrochloride under AM 1.5 illumination. (c) Digital photos show simultaneous hydrogen and electricity generation of the SMPP system during degrading tetracycline hydrochloride under simulated sunlight. (d) Degradation of tetracycline hydrochloride by the SMPP system under AM 1.5 illumination for five repeat times. (b) shows that the SMPP system has a steady current density and hydrogen generation rate during degrading tetracycline hydrochloride, which further demonstrates the stability of the SMPP system for longtime application. The average current density is 2852 $\mu\text{A cm}^{-2}$, and the average hydrogen generation rate is 52.6 $\mu\text{mol h}^{-1} \text{cm}^{-2}$. This result demonstrates the SMPP system can not only efficiently purify wastewater but also simultaneously supply electricity and hydrogen using sunlight, which is further illustrated by the digital photos shown in Fig. 7c. Fig. 7d shows the degradation of tetracycline hydrochloride by the SMPP system under AM 1.5 illumination for five repeat times. It can be seen that the removal ratio of tetracycline hydrochloride in every 3 h operation was in the range of 89–91%, which confirms the excellent stability of SMPP system for longtime application. A slow reduction of the treatment efficiency of the SMPP system was observed at the earlier repeat uses, which may be due to the passivation of some unstable active sites on the photoanode caused by possible photocorrosion or irreversible adsorption [23].

Table 1

Comparison with others energy recovery system of PFC in electric production.

| Configuration | Light source | Substrate | J_{sc} ($\mu\text{A cm}^{-2}$) | V_{oc} (V) | JV_{max} ($\mu\text{W cm}^{-2}$) | P_{max} ($\mu\text{W cm}^{-2}$) | Refs. |
|---|---------------|----------------------------|---------------------------------------|-----------------|---|--|-----------|
| TiO ₂ + Pt | AM 1.5 | Phenol | 320 | 1.49 | 230 | – | [5] |
| WO ₃ + Cu ₂ O | AM 1.5 | Phenol | 205 | 0.33 | 68 | – | [8] |
| WO ₃ + Pt/PVC | AM 1.5 | Methylene blue | 350 | 0.38 | 133 | – | [9] |
| BiVO ₄ /WO ₃ + Pt/BJS | AM 1.5 | Glucose | 350 | 0.82 | 287 | – | [10] |
| W:BiVO ₄ + pTTh | AM 1.5 | Glucose | 775 | 0.62 | 481 | 82 | [12] |
| TiO ₂ + C/Cu ₂ O | AM 1.5 | Phenol | 500 | 0.41 | 205 | 73 | [11] |
| CdS + Cu ₂ O | AM 1.5 | Phenol | 310 | 0.62 | 192 | 60 | [11] |
| TiO ₂ + Ag/TiO ₂ | 500 W Xe lamp | Acidic water | 57 | 1.59 | 91 | 11 | [31] |
| TiO ₂ + BiOCl | 500 W Xe lamp | Acidic water | 71 | 1.69 | 120 | 16 | [32] |
| TiO ₂ + Cu ₂ O | AM 1.5 | Glucose | 230 | 0.49 | 113 | 36 | [33] |
| SMPP | AM 1.5 | tetracycline hydrochloride | 2900 | 1.35 | 3915 | 1112 | This work |

(pTTh) photocathode was recently reported [12], outperforming that of PFCs previously reported. However, it is only 7.4% of that of this work, which means the electricity output of the SMPP system is nearly 14 times that of the PFC. This marvelous improvement in electricity output efficiency can be due to the enhanced sunlight exploitation and the good energy conversion property of the rear Si PVC, which demonstrates the superiority of the novel SMPP system for wastewater recycling compared the reported systems such as PFC.

Fig. 7b shows that the SMPP system has a steady current density and hydrogen generation rate during degrading tetracycline hydrochloride, which further demonstrates the stability of the SMPP system for longtime application. The average current density is 2852 $\mu\text{A cm}^{-2}$, and the average hydrogen generation rate is 52.6 $\mu\text{mol h}^{-1} \text{cm}^{-2}$. This result demonstrates the SMPP system can not only efficiently purify wastewater but also simultaneously supply electricity and hydrogen using sunlight, which is further illustrated by the digital photos shown in

Table 2
Performance of the SMPP system using various organics.

| Model pollutants | J_{sc} ($\mu A\ cm^{-2}$) | V_{oc} (V) | P_{max} ($\mu W\ cm^{-2}$) | H_2 generation rate ($\mu mol\ h^{-1}\ cm^{-2}$) | Removal rate after 3 h (%) | TOC removal rate after 3 h (%) |
|--|----------------------------------|-----------------|-----------------------------------|---|----------------------------|--------------------------------|
| Methylene blue (10 mg L ⁻¹) | 2243 | 1.28 | 964 | 45.7 | 98.1 | 53.5 |
| Congo Red (10 mg L ⁻¹) | 2326 | 1.31 | 991 | 47.2 | 97.2 | 46.8 |
| Phenol (10 mg L ⁻¹) | 2851 | 1.36 | 1145 | 52.5 | 82.3 | 49.1 |
| Bisphenol A (10 mg L ⁻¹) | 2812 | 1.35 | 1134 | 51.8 | 78.7 | 44.2 |
| p-chlorophenol (10 mg L ⁻¹) | 2763 | 1.34 | 1098 | 50.9 | 75.2 | 45.6 |
| Oxytetracycline (10 mg L ⁻¹) | 2874 | 1.36 | 1158 | 52.9 | 92.5 | 59.4 |
| Urea (20 mg L ⁻¹) | 3255 | 1.30 | 1544 | 59.7 | 99.5 | 91.4 |
| Dimethyl formamide (20 mg L ⁻¹) | 3112 | 1.29 | 1487 | 57.3 | 96.2 | 77.3 |
| Acetic acid (20 mg L ⁻¹) | 3483 | 1.34 | 1846 | 64.9 | 98.1 | 81.5 |
| Mannitol (20 mg L ⁻¹) | 3299 | 1.31 | 1627 | 60.8 | 95.6 | 63.2 |

Fig. 7c. Fig. 7d shows the degradation of tetracycline hydrochloride by the SMPP system under AM 1.5 illumination for five repeat times. It can be seen that the removal ratio of tetracycline hydrochloride in every 3 h operation was in the range of 89–91%, which confirms the excellent stability of SMPP system for longtime application. A slow reduction of the treatment efficiency of the SMPP system was observed at the earlier repeat uses, which may be due to the passivation of some unstable active sites on the photoanode caused by possible photocorrosion or irreversible adsorption [23].

The performance of the SMPP system for degrading organics and simultaneous clean energy production was further investigated by using various organics as model substrates under simulated sunlight illumination (Table 2). The J - V characteristics were obtained at the initial stage. The H_2 generation rate was the average value in 3 h operation. As shown in Table 2, for refractory organic matters, the removal rates of organic dyes, such as methylene blue (MB) and Congo red (CR), are higher than phenolic compounds, such as phenol, bisphenol A (BPA) and p-chlorophenol (CP), while their H_2 generation rate are lower, except oxytetracycline (OTC) with a relatively higher removal rate (92.5%) and H_2 generation rate ($52.9\ \mu mol\ h^{-1}\ cm^{-2}$). However, when using some non-refractory organic matters, such as urea, dimethyl formamide (DMF), acetic acid and mannitol, the electricity output and hydrogen evolution rate are both improved, and the removal rates are also higher than the system with refractory organic matters. This could be due to the simple structures of these non-refractory organic matters, which are easy to be oxidized by photogenerated holes or hydroxyl radicals [34]. For example, the SMPP system with acetic acid shows a H_2 generation rate of $64.9\ \mu mol\ h^{-1}\ cm^{-2}$ and a removal rate of 98.1%. However, the removal rate is an apparent parameter of the target contaminant, which cannot reflect the mineralization of organic pollutants. Therefore, total organic carbon (TOC) removal rate in each system was further calculated after 3 h operation (Table 2). The result indicates that the removal rate of TOC is lower than that of the target contaminant, and the non-refractory organic matters show higher TOC removal rates than refractory organic matters. Although the removal rates of MB and CR are 98.1% and 97.2%, respectively, their TOC removal rates are only 53.5% and 46.8%, respectively. This may be due to their easy discolorization by the attack of hydroxyl radicals, while their intermediate productions that have benzene ring structures are relatively stable and refractory to decompose [35]. Their relatively lower H_2 generation rates may be due to the photons' losses absorbed by the organic dyes. For OTC, its relatively higher removal rate than

other phenolic compounds may be due to its reducibility from alcoholic extract hydroxyl group, which can be easily oxidized by photo-generated holes and hydroxyl radicals, while its relatively low TOC removal rate may be attributed to its benzene ring structure. However, the TOC removal rate of urea reaches 91.4%, which may be due to its single carbon structure that can be easily oxidized into carbon dioxide. Although the performance of the SMPP system is varied when using different organic substrates, the experimental data in Table 2 provides compelling support for the suitability of the SMPP system for producing clean energy while simultaneously photodecomposition of a large variety of organic waste.

The cost of the SMPP system is also an important factor that affect its large-scale application. Taking the SMPP system ($4 \times 2\ cm^2$) tested in this work as an example, this system includes five main parts: photoanode, Si PVC array, wire, sealant, and cathode. The cost of the $WO_3/BiVO_4$ photoanode ($4 \times 2\ cm^2$) is approximate 0.96 dollar after checking the consumption of every reagent and FTO glass as shown in the experimental part. The commercial Si PVC array ($4 \times 2\ cm^2$, Shenzhou New Energy Development Co., Ltd., China) is approximate 0.47 dollar. The cost of wire and sealant is almost negligible. The Pt-black/Pt cathode ($1 \times 1 \times 0.01\ cm^3$) is relatively costly (~23 dollars, Shanghai INESA Scientific Instrument Co., Ltd, China). Therefore, the SMPP system used in this work costs approximate 24.43 dollars. However, when applied in large scale, the cost of photoanode and Si PVC array will decrease because the unit prices of materials will be reduced in large amount. Furthermore, the Pt-black/Pt cathode can be replaced by relatively cheap Pt/C cathode (approximate 0.18 dollar cm^{-2} , Shenzhou New Energy Development Co., Ltd., China) or non-noble metal catalyst such as Nickel compounds or metal sulfide. Therefore, the cost of SMPP system will be less than 0.2 dollar cm^{-2} ($8\ cm^2$ photoanode, $8\ cm^2$ PVC array and $1\ cm^2$ Pt/C cathode) when using in large-scale. In addition, the SMPP system can operate under sunlight illumination while without any other energy consumption. In general, the SMPP system is a relatively cheap and economical way for producing clean energy while simultaneously wastewater treatment.

3.4. Environmental applications of a SMPP system

As aforementioned, water pollution has become a world-wide problem that causes terrible threaten to natural system and human health [1,2]. For example, trace levels of antibiotics in waters can cause the rise of antibacterial activity, pathogen antibiotic resistance, and toxicity

to the downstream environments, therefore presenting both an ecosystem and human health risk [36]. However, antibiotics (and also other toxic and refractory organic waste, such as organic dyes and phenolic compounds) are hardly to be degenerated by conventional water and wastewater treatment technologies [37,38], and effective antibiotic treatment technologies, such as reverse osmosis or advanced oxidation processes, are typically energy intensive ($1 \sim 10 \text{ kWh m}^{-3}$) [39], which are not suitable for large-scale water remediation, such as rivers and lakes [40]. In this case, a SMPP system can be a strong candidate to remediate such kinds of waters, even in rural areas or developing countries, because it can be constructed as a compact and large-scale device that can efficiently remove organic pollutants and simultaneously output electricity and hydrogen as energy supplier for local residents under sunlight.

4. Conclusion

In summary, a novel SMPP system that consisted of a high-performance $\text{WO}_3/\text{BiVO}_4$ photoanode, a rear Si PVC and a Pt-black/Pt cathode was proposed for efficiently producing clean energy from refractory organics degradation. The heterostructured $\text{WO}_3/\text{BiVO}_4$ photoanode showed evidently enhanced PEC performance compared with the WO_3 photoanode. The J - V characters of the rear Si PVC affected the performance of the SMPP system. The optimal SMPP system shows an efficient and stable degradation of tetracycline hydrochloride with a rate constant of 0.75 h^{-1} , and yields the V_{oc} of 1.35 V, J_{sc} of $2900 \mu\text{A cm}^{-2}$, P_{max} of $1112 \mu\text{W cm}^{-2}$, and hydrogen generation rate of $52.6 \mu\text{mol h}^{-1} \text{ cm}^{-2}$. The electricity output of the SMPP system is nearly 14 times that of the ultimate PFC system to date. Furthermore, various refractory organics can be used as substrates for the SMPP system. All the results suggested that the proposed SMPP system is believed to provide a novel efficient way to simultaneously purify wastewater and produce clean energy under sunlight.

Acknowledgements

The authors would like to acknowledge National Key Research and Development Plan (2016YFA0203200), the National Natural Science Foundation of China (51538013), the Natural Science Foundation of Guangdong Province (2018A030313367 and 2018A030313487) and the Science Starting Foundation of Guangzhou University (69–18ZX10298, 27000503151 and 2700050302) for financial support.

References

- [1] J. Snape, C. Lewis, R. Murray-Smith, *Nature* 477 (2011) 33.
- [2] R. Stone, *Science* 333 (2011) 1210–1211.

- [3] W.-W. Li, H.-Q. Yu, B.E. Rittmann, *Nature* 528 (2015) 29–31.
- [4] M. Kaneko, J. Nemoto, H. Ueno, N. Gokan, K. Ohnuki, M. Horikawa, R. Saito, T. Shibata, *Electrochem. Commun.* 8 (2006) 336–340.
- [5] Y. Liu, J. Li, B. Zhou, H. Chen, Z. Wang, W. Cai, *Chem. Commun.* 47 (2011) 10314–10316.
- [6] P. Lianos, *J. Hazard. Mater.* 185 (2011) 575–590.
- [7] B. Seger, G.Q. Max, L. Lu, Wang, J. *Mater. Chem.* 22 (2012) 10709–10715.
- [8] Q. Chen, J. Li, X. Li, K. Huang, B. Zhou, W. Cai, W. Shanguan, *Environ. Sci. Technol.* 46 (2012) 11451–11458.
- [9] Q. Chen, J. Bai, J. Li, K. Huang, X. Li, B. Zhou, W. Cai, *Chem. Eng. J.* 252 (2014) 89–94.
- [10] Q. Zeng, J. Bai, J. Li, Y. Li, X. Li, B. Zhou, *Nano Energy* 9 (2014) 152–160.
- [11] Z. Wu, G. Zhao, Y. Zhang, J. Liu, Y. Zhang, H. Shi, J. *Mater. Chem. A* 3 (2015) 3416–3424.
- [12] B. Zhang, W. Fan, T. Yao, S. Liao, A. Li, D. Li, M. Liu, J. Shi, S. Liao, C. Li, *ChemSusChem* 10 (2017) 99–105.
- [13] H. Liu, H. Liu, R. Ramnarayanan, R. Ramnarayanan, B.E. Logan, B.E. Logan, *Environ. Sci. Technol.* 38 (2004) 2281–2285.
- [14] Q. Zeng, J. Li, J. Bai, X. Li, L. Xia, B. Zhou, *Appl. Catal. B Environ.* 202 (2017) 388–396.
- [15] Q. Zeng, J. Li, L. Li, J. Bai, L. Xia, B. Zhou, *Appl. Catal. B Environ.* 217 (2017) 21–29.
- [16] M. Sadakane, K. Sasaki, H. Kunioku, B. Ohtani, R. Abe, W. Ueda, *J. Mater. Chem.* 20 (2010) 2092–2100.
- [17] S. Tokunaga, H. Kato, A. Kudo, *Chem. Mater.* 13 (2001) 4624–4628.
- [18] Y. Pihosh, I. Turkevych, K. Mawatari, T. Asai, T. Hisatomi, J. Uemura, M. Tosa, K. Shimamura, J. Kubota, K. Domen, T. Kitamori, *Small* 10 (2014) 3692–3699.
- [19] M. Zhou, J. Bao, Y. Xu, J. Zhang, J. Xie, M. Guan, C. Wang, L. Wen, Y. Lei, Y. Xie, *ACS Nano* 8 (2014) 7088–7098.
- [20] F.F. Abdi, T.J. Savenije, M.M. May, B. Dam, R. Van De Krol, *J. Phys. Chem. Lett.* 4 (2013) 2752–2757.
- [21] I. Grigioni, K.G. Stamplecoskie, E. Selli, P.V. Kamat, *J. Phys. Chem. C* 119 (2015) 20792–20800.
- [22] K. Miyake, H. Kaneko, M. Sano, N. Suedomi, *J. Appl. Phys.* 55 (1984) 2747–2753.
- [23] T.W. Ng, L. Zhang, J. Liu, G. Huang, W. Wang, P.K. Wong, *Water Res.* 90 (2016) 111–118.
- [24] Z. Jin, Z. Hu, J.C. Yu, J. Wang, *J. Mater. Geosci.* 4 (2016) 13736–13741.
- [25] Z. Wei, J. Hu, K. Zhu, W. Wei, X. Ma, Y. Zhu, *Appl. Catal. B Environ.* 226 (2018) 616–623.
- [26] O. Carp, C.L. Huisman, A. Reller, *Prog. Solid State Chem.* 32 (2004) 33–177.
- [27] W.H. Koppenol, J.F. Liebman, *J. Phys. Chem.* 88 (1984) 99–101.
- [28] C. Hu, T. Peng, X. Hu, Y. Nie, X. Zhou, J. Qu, H. He, *J. Am. Chem. Soc.* 132 (2010) 857–862.
- [29] A. Shang, X. Li, *Adv. Mater.* 29 (2016) 1603492.
- [30] J. Liu, H. Xu, Y. Xu, Y. Song, J. Lian, Y. Zhao, L. Wang, L. Huang, H. Ji, H. Li, *Appl. Catal. B Environ.* 207 (2017) 429–437.
- [31] Y. Ogura, S. Okamoto, T. Itoi, Y. Fujishima, Y. Yoshida, Y. Izumi, *Chem. Commun. Camb.* 50 (2014) 3067–3770.
- [32] Y. Fujishima, S. Okamoto, M. Yoshida, T. Itoi, S. Kawamura, Y. Yoshida, Y. Ogura, Y. Izumi, *J. Mater. Chem. A* 3 (2015) 8389–8404.
- [33] J. Li, J. Li, Q. Chen, J. Bai, B. Zhou, *J. Hazard. Mater.* 262 (2013) 304–310.
- [34] Q. Zeng, J. Bai, J. Li, L. Li, L. Xia, B. Zhou, *Appl. Energy* 220 (2018) 127–137.
- [35] M.N. Chong, B. Jin, C.W.K. Chow, C. Saint, *Water Res.* 44 (2010) 2997–3027.
- [36] Q.Q. Zhang, G.G. Ying, C.G. Pan, Y.S. Liu, J.L. Zhao, *Environ. Sci. Technol.* 49 (2015) 6772–6782.
- [37] Y. Liu, Q. Yao, X. Wu, Y. Ma, C.N. Ong, J. Xie, *Nanoscale* 8 (2016) 10145–10151.
- [38] Q. Sui, J. Huang, S. Deng, W. Chen, G. Yu, *Environ. Sci. Technol.* 45 (2011) 3341–3348.
- [39] I. Michael, L. Rizzo, C.S. McArdell, C.M. Manaia, C. Merlin, T. Schwartz, C. Dagot, D. Fatta-Kassinos, *Water Res.* 47 (2013) 957–995.
- [40] J. Wang, S. Wang, *J. Environ. Manage.* 182 (2016) 620–640.